



A Geospatial Analysis and Kernel Density Estimation of River Quality Parameter in Bulacan, Philippines

Jayson M. Victoriano¹, Luisito L. Lacatan²

¹AMA University-Quezon City, Philippines, jaysonv14@yahoo.com

² Dean of College of Engineering at AMA University-Quezon City, llacatan@amaes.edu.ph

ABSTRACT

This study intends to visualize the water quality using different parameters in determining the river pollution in the province of Bulacan with the use of Geographic Information System (GIS) together with Kernel Density Estimation (KDE). Utilizing the different water quality parameters like Dissolved Oxygen (DO), Potential of Hydrogen (pH), Biochemical Oxygen Demand (BOD), Total Suspended Solids (TSS), Nitrate, Phosphate, and Coliform is the premise in deciding the water quality level. The information considered reliably based on the given historical data gathered from January 2013 to May 2018. In this regard, the GIS model shows the hotspot area of the diverse water quality parameters and Water Quality Index (WQI). By employing the Predictive Accuracy Index (PAI) also helps to measure how accurate the spatial distribution produced by the GIS model. As a result, the majority of the sampling station is polluted, provided that they have 'Poor' and 'Very Poor' condition.

Key words: River Pollution, GIS, Water Quality Index, and Kernel Density Estimation.

1. INTRODUCTION

In the Philippines, Marilao-Meycauayan-Obando River System (MMORS) is infamous for its reputation as one of the "World's Worst Polluted Places," as declared by Pure Earth in 2007 also known as Blacksmith Institute [1]. According to Malenab et al. [2], heavy metal pollution came from used jewelry smelting, tanneries, used lead-acid battery recycling and other industries dealing with heavy metals are one of the commonly found pollutants in the upper area of the river system. These contaminants, most especially heavy metals, pose a significant health risk to nearby communities that surround the river water for fish ponds, bathing, and swimming that causes some health concerns, and also, 31% of all diseases in the nation are ascribed to contaminated waters. 5 out of 10 Filipinos for each day experience maladies attributed to poor sanitation and poor water quality. There are several attempts to rehabilitate the river, and the noteworthy one that should be credited to the ongoing MMORS

rehabilitation actions is the compliance of many industries, which started in 2008, as of adherence with the DENR declaration the river system as a Water Quality Management Area (WQMA). Figure. 1 shows the observed condition of MMORS and its surroundings.



Figure 1: Water Condition around MMORS

The substantial data (water quality parameter) such as DO, pH, BOD, TSS, Nitrate, Phosphate, and Coliform are collected from January 2013 to May 2018.

Figure 2 show the map of MMORS and its sampling stations covering around 55 kilometers from upstream Caloocan down to Manila Bay.

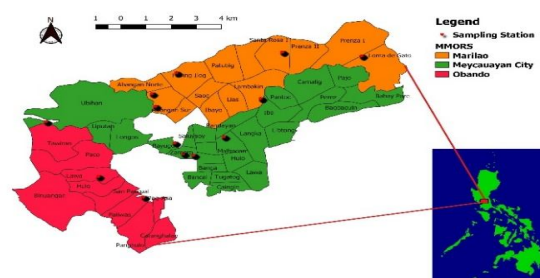


Figure 2: Study Area - MMORS

The main objectives solved in this case study are analyzed and achieved through a series of procedures before determining the pollution level. Initially, to visualize the heatmap area, the GIS model is used hand-in-hand with KDE. KDE utilized the data mining technique to extract the featured river quality parameter in evaluating the river. After these procedures, the PAI is established which is a way of

measuring the reliability and accuracy of a specific heat mapping technique in making a hotspot map output where a potential pollution area may be dense. In the end, the most precise heatmap is devised that represents conditions useful for future reference concerning river pollution.

2. PROCEDURE

2.1 Study Area

The study is conducted on three coastal municipalities in Bulacan (Figure. 2). Thirteen sampling stations composing of almost five barangays in Marilao, another five barangays in Meycauayan, and three nearby areas in Obando, all in the province of Bulacan, Philippines are included in the study using cluster sampling design.

2.2 Preprocessing

The collected dataset is based on the Department of Environment and Natural Resources (DENR) Environment Management Board (EMB) Region 3 and applied data mining techniques of aggregating and scrubbing [3] feature data parameters for the river, starting from January 2013 to May 2018.

This included the different water parameters and standards, as shown in Table I. In conjunction with is Table II which provides the water quality index following the international standard of water quality and acceptable with the DENR-EMB standards. The authors focused on DO, pH, BOD, TSS, Nitrate, Phosphate, and Coliform [4] [5] that measures the water quality of the river. These are parameters of biodegradable organic matter that are generally used to ascertain threshold in terms of potability of river water. Based on the Water Quality Guideline of DENR Administrative Order[6], MMORS is classified as a Type C body of water.

Table 1: Water parameter and standard [6]

Parameter	Standard
DO	5 mg/l
pH	6.5-8.5 mg/l
BOD	7 mg/l
TSS	80 mg/l
Coliform	7 mg/l
Nitrate	7 mg/l
Phosphates	0.5 mg/l

Table 2: General Description of the Calculated Water Quality [4] [7] [11].

WQI Value	Water Quality
>=90	Excellent
>=70	Good
>=50	Poor
>=25	Very Poor
>=0	Worst

2.3 Water Quality Index

This study is calculated following three steps using various water quality parameters [7][8][9][10]. For the first step, an observed weight (*w_i*) is to be assigned in between each of the seven (7) indispensable parameters that must be regarded according to its distinct and unique attributes that contributed to the overall quality of river water. After this step, another procedure is to compute relative weight (*W_i*) as shown in equation 1:

$$W_i = \frac{w(i)}{\sum_{i=1}^n w_i} \quad (1)$$

where: (*W_i*) signifies the relative weight dedicated to each of the water quality parameters, on the contrary (*w_i*) is the actual weight for every parameter, and lastly, (*n*) is the number of absolute parameters set and completed. For the last advance, a quality rating scale (*q_i*) for every parameter is being appointed by isolating its fixation in each water test and as indicated by its separate standard and the outcome at long last is increased by 100 to express it in rate shown in equation 2.

$$q_i = \frac{C_i}{S_i} * 100 \quad (2)$$

where: (*q_i*) is the quality rating, (*c_i*) is the centralization of every pollution in the water, sub-indices (*S_i*) were first calculated for each parameter is shown in equation 3. and then calculate the WQI shown in equation 4:

$$S_i = W_i * q_i \quad (3)$$

$$WQI = \sum_{i=1}^n S_i \quad (4)$$

2.4 Geographic Information System Model

Geographic Information System (GIS) is considered as one of the first electronic information system used to virtually and visually represent and to set forth the analysis of the geographic features present on the Earth's surface [12] [13]. With certain advancements, GIS innovation can implant regular database tasks, for example, question and measurable investigation with cutting edge representation and geographic examination benefits offered by maps [14]. Also, it is being used to make a digital reproduction for the earth's surface and the events that take place on it. This study uses QGIS 3.2 Bonn version.

There is a diverse selection of mapping techniques that can be implemented for easy determination and exploration of patterns of water pollution [15], particularly in terms of water quality showed in Figure 3. Among those mentioned in this study, the researcher considers the Kernel Density Estimation (KDE) to be one of the undisputed hotspot mapping methods to be utilized in determining spatial clusters of pollution through the scrutiny of the trends among the mapping techniques illustrated below.

2.5 Kernel Density Estimation

There are several available spatial analysis techniques out in the market that can be employed for identification of prospective hotspots, but among all of these techniques in the recent years, KDE is the most popular and regard as the mainstream technique if talking about spatial analysis [16] [17] [18] [19] KDE (Gaussian Function) is calculated by weighting the distances of all the data points for each location on the line.

The concept of weighting the distances of observations from a particular point χ , can be expressed mathematically using equation 5:

$$f(h)(x) = 1/nh * \sum_{i=1}^n K((x-x_i)/h) \quad (5)$$

wherein $K(\chi)$ denotes the kernel function that as a rule is smooth, it is intertwined with symmetric function, for instance, is a Gaussian, and $h > 0$ is known as the smoothing data transfer capacity that controls the measure of smoothing. The KDE facilitates every data point X_i into small density bumps and sum all these small bumps together to accomplish the final estimation.

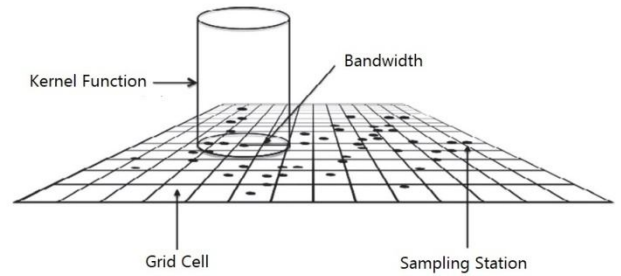


Figure 4: KDE Visual Process [17]

Figure. 4 shows how the KDE process visually, KDE begins by overlaying a two-dimensional system over an entire study area. One of the principal parameters that must be set up, as such, is the manner by which enormous to make each cell. Decision rules about grid cell size or the number of areas into which the system overlay will be isolated are regularly founded on the amount of the study region. KDE maps with more prominent goals (for example less pixilation) are delivered from network overlays with littler cells (for example more sections), even though maps with less objectives result when system overlays are incorporated higher estimated cells (for example fewer sections) Grid cell size may have important indication on how effective KDE maps are.

2.6 Validation

On a different note, the accuracy will be measured using the Prediction Accuracy Index (PAI). Based on the Ratclief and Chainey study [15] [20], the PAI is a way of measuring if the reliability and also the accuracy of a heatmapping technique make a precise output to where exactly pollution may be dense with a known area. One of the highlights of its measurement protocols to take account areas that might differ from heatmap to heatmap. If a heatmap can cover a wide range of a specified area and all the potential pollution is in the area of that concentrated heatmap, for some it might appear as if it is like a good outcome, even though in reality it is not. In this study, the PAI will be used to see how the results differ. The PAI is determined dependent on the determined region and the essential hit, to convey a progressively exact result of how precise the heatmap [16] actually is. The PAI is determined by partitioning the hit rate by the area rate, the zone of the hotspots in connection to the entire study area. For better understanding, see equation 6 below.

$$(n/N) * 100 / ((a/A) * 100) = PAI \quad (6)$$

n : it is the number of accumulated amount of pollutions in specific areas where certain pollutants are anticipated to occur (e.g. hotspots) N : number of pollutions in concerned area a : stands for area (e.g. km²) of assigned areas where pollutions are predicted and subject to occur (e.g. area of hotspots) A : area (e.g. km²) of the study area.

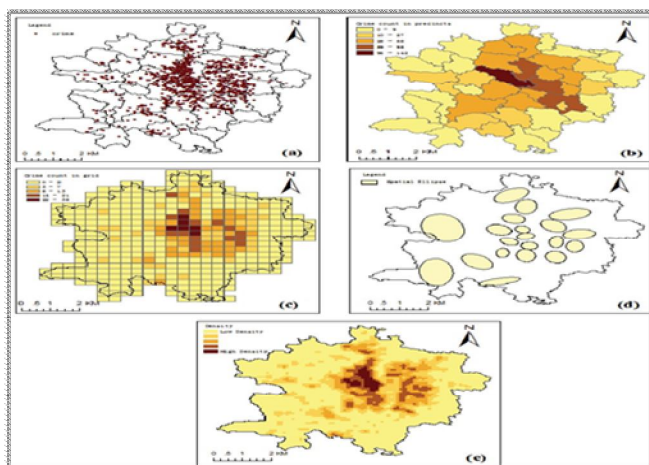


Figure: 3 Conventional hotspot mapping techniques. (a) Point mapping, (b) choropleth thematic map, (c) grid thematic mapping, (d) standard deviational spatial ellipses and (e) KDE. [15]

3. RESULTS

In this section, a summary of the spatial distribution for the 7 water quality parameter and WQI result in a heat map interpolation representation is illustrated. Also, a PAI result that would be used to determine which is much accurate in terms of heat map interpolation selection.

3.1 Water Quality Index

Figure. 5 shows the water quality index result for the study area from 2013 up to 2018. The weighted data show how the river behaves during each year and to check the categorical level, and Table II explains the WQI value of the river.

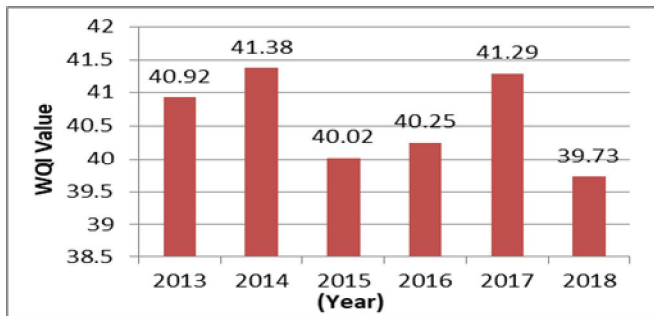


Figure 5: WQI result

3.2 Predictive Accuracy Index

Table III shows the PAI results after implementing different cell sizes fitted on KDE hotspot maps for MMORS sampling stations. The PAI results for the water quality parameter varied depending on the grid cell size.

Table 3: Prediction Accuracy Index Result [17]

	150 Columns/Grid Cell	250 Columns/Grid Cell	300 Columns/Grid Cell
Mean	9.91	16.51	19.64

For instance, the grid cell of 150 meters with a mean value of 9.91, 250m with the mean value of 16.51 and 300m with the mean value of 19.64, respectively. These results not only suggest that PAI values gradually increase as the grid cell size increases but also its difference can still be marginal. These results also imply that the PAI at a higher level alludes to the possibility of the more exceptional ability of the hotspot map to produce accurately. It simply means the most accurate grid cell and bandwidth fit for this study is the highest value of 300m which is shown in Table III. The smoothing bandwidth that is perfect and more accurate in this hotspot map is 1.7 meters.

3.3 Spatial Distribution

Biochemical oxygen demand or commonly known as BOD is among chemical substances monitored in determining the tolerable amount of dissolved oxygen necessary for aquatic organisms in a body of water that somehow breaks down organic material that must be existent not just in a given water sample contemplated in this undertaking at a certain temperature over a particular timeframe.

Figure. 6 shows the spatial distribution of BOD generated using the GIS model. There is a clear variation at some point in the heat map considering each of the sampling stations. It is evident in the distribution that there is indeed a gradual decrease and increase of such substance when crossing the river system from both ends toward the center or the other way around.

From Figure. 6, the BOD is low in most of the area of Marilao, mainly in Santa Rosa I, Prenza I and II. The high concentration of BOD is found in the river areas of Malhacan, Zamora, Saint Francis and part of nearby sampling stations. This is above the desirable limit of BOD concentration in river water. The BOD should fill in as a pointer of the measure of putrescible natural issue present in water. Along these lines, a low BOD is an indicator of good quality water, while a high BOD shows contaminated water.

Another vital indicator which is dissolved oxygen in water can only be established if free O₂ molecules are existing within the water. Thus, the simply puts bonded oxygen molecule which can likewise be existing in water (H₂O) is in a compound and doesn't check toward broke up oxygen levels.

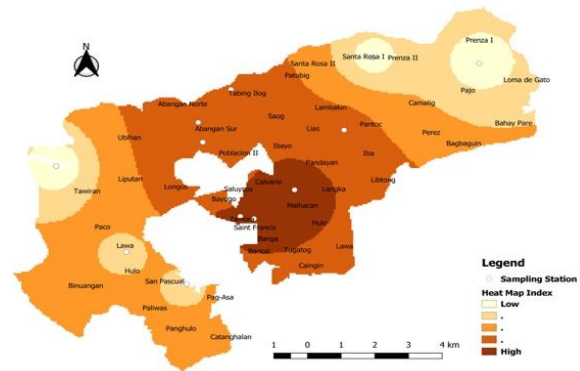


Figure 6: BOD Spatial Distribution

To have a clearer picture of this parameter, if one tries to picture out similarities of oxygen molecules being dissolved in water are most likely the same manner on how salt or sugar does when it is stirred.

The findings in this parameter show that the spatial distribution for Dissolve Oxygen fluctuates heavily in the extremities of MMORS in Figure. 7 with the aid of GIS. The

substantial transition between the two is further expounded in Figure. 7, where the water parameter set off higher intensity at the margins of the river system.

From Figure. 7, in connection or contrary to Figure.6, Malhacan, Zamora, and Saint Francis in Meycauayan, Santa Rosa I, Prenza I and II in Marilao and some close by stations in the stated river areas are below and above the desirable limit of DO respectively. The remaining stations of MMORS within limits. If low dissolved oxygen can cause problems same goes with high concentrations. When this condition occurred, supersaturated water can lead to gas bubble disease to mostly fish and some invertebrates. In some cases, a body of water with recognizable high concentrations of dissolved minerals such as salt may indicate a lower DO concentration when compared to freshwater with the same condition. Also, there is evidence that low dissolved oxygen (DO) in the waters may primarily yield to excessive algae outgrowth caused by phosphorus substances. Also, nitrogen is another nutrient that can contribute to algae growth.

Unlike all other indicators or parameters such as temperature and dissolved oxygen, the apparent presence of nitrates in a body of water usually does not have a direct effect on marine species like that of insects or fish. However, if excess levels of nitrates in water are investigated it can create conditions that make it difficult for the aforementioned organisms to survive and to sustain life underwater. Although there are isolated cases wherein nitrates are used as a source of food similar to algae and other plants.

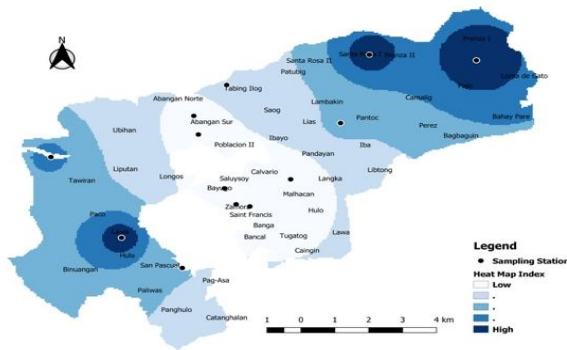


Figure 7: DO Spatial Distribution

In this water quality parameter, the density estimates by means of spatial distribution drawn a quite difference which is patent in the next Figureure. Figure. 8 insinuates the diminution of the water substance from the upper right borders of MMORS down to lower limits. This only denotes that this is one of the parameters that should be given much attention in undertaking water quality.

From Figure. 8, the nitrate concentration in the examined area of the river water is within the allowable limit (<45mg/l) if we are going to observe the permissible threshold. This would only mean that nitrate concentration in between 45-100 mg/l is mostly in the sampling stations of Marilao like Loma De Gato, Camalig, Patubig, Santa Rosa II, Tabing Ilog, Abangan Norte, etc. Higher nitrate concentrations of more

than 100 mg/lit are found in areas like Santa Rosa I, Prenza I and II in Marilao which is very similar to the BOD level.

Coliform bacteria are typically present in an environment wherein all warm-blooded animals and humans reside and produce feces. Even though coliform bacteria are unlikely to cause illness, but their mere presence not just in drinking water per se insinuates that high risk or probability of disease-causing organisms (pathogens) could be in the water system.

Based on Figure. 9, the coliform spatial distribution alludes approximately half of water sampling stations are more or less polluted with this kind of substance. This only implies that the actual estimation for coliform and, in reality, are not at far from each other; therefore, accuracy is achieved.

Figure. 9 shows, except Zamora, Saint Francis, and surrounding areas, the remaining stations of MMORS in terms of coliform water are somehow moderate and low. However, from the map below, predominantly areas river water quality within Marilao and Meycauayan are still doubtful. This would only indicate the potential presence of disease-causing bacteria in water. Furthermore, it might also suggest that human or animal waste is entering the water supply.

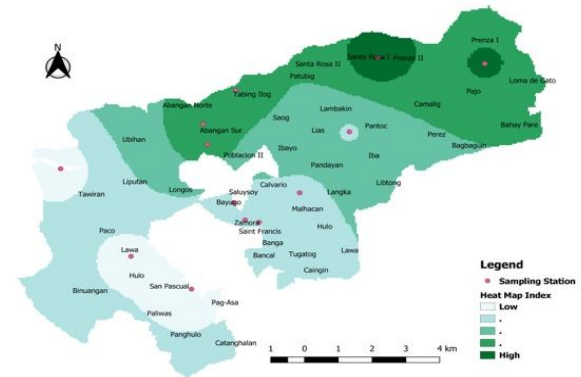


Figure 8: Nitrates Spatial Distribution

Studies suggest that pH value as an indicator is useful to countercheck whether water is potable to drink or not not especially for households or daily. As a standard, a pH of pure water is 7 and this is being compromised globally. Generally speaking, specific water with a pH lower than 7 it is considered and said to be acidic, and with a pH more prominent than 7 is viewed as essential correspondingly. The acknowledged range for pH in surface water frameworks is 6.5 to 8.5, and on this occasion, the apparently ordinary pH goes for waterway water frameworks is between 6 to 8.5.

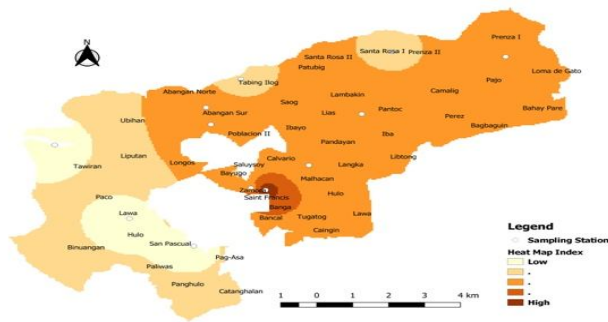


Figure 9: Coliform Spatial Distribution

The estimation of the point of confinement of the water to contradict an alteration in pH that would will, all in all, make the water continuously acidic is called alkalinity. Both investigations of alkalinity and pH are considered basic to decide the harmfulness of the water.

To ascertain the pH using GIS, the researcher devised the spatial distribution which can be observed in Figure. 10 across all the sampling stations. In a similar Figureure, it tends to be seen that the spreading of this parameter intensifies as one moved to the edges of the map. This only reveals that there is a close association with this parameter and the other ones.

From Figure. 10, a considerable number of sampling stations in Obando and Marilao river areas such as Tawiran, Lawa, Loma De Gato, Santa Rosa I, Prenza I and II have above the permissible limit i.e., neutral pH of 7. The lower concentration of pH is found to be within the sampling stations primarily in Meycauayan. This only suggests that zero through 7 shows acidity; the lower the number the higher the corrosiveness. Consumption of too much acid in our body is indeed harmful and, in a worst-case scenario, detrimental as warned by the Environmental Protection Agency (EPA). As prescribed by medical practitioners, potable drinking water that is safe to drink must, at any rate, have a pH estimation of 6.5-8.5 to fall inside EPA measures, and they significantly further note that the given satisfactory pH go, be it somewhat high-or low-pH water can be unappealing for a few reasons.

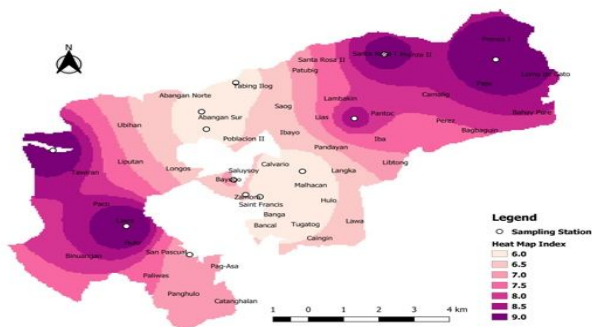


Figure 10: pH Spatial Distribution

Phosphate in bodies of water is one of the most essential elements that must be present for river plant life, but when there is unwarranted amount of it in water, it can really speed up the process so-called eutrophication (a chemical means of reducing dissolved oxygen particularly in water bodies which is the result of caused by an increase of mineral and organic nutrients) that can be observed mostly amongst rivers and lakes. Another major contributor of phosphorus manifestation to rivers is soil erosion.

The lower frame, which in Figure. 11, displays the spatial distribution for Phosphates. The map also shows the progressive dispersal of the substance at some of the points that indicate convergence. There is a slight disparity at some point but there is a critical junction at the end of the heat map.

From Figure. 11, the river water phosphate among the sampling stations in Obando is within the desirable limits. On the other hand, sampling stations, for instance, Lias, Tabing Ilog, Abangan Norte and Sur in Marilao are at concentrations above the permissible limits for potable water quality. Although a high level of phosphate may impressively lead to a sudden increase in terms of fish population and eventually improve the overall water quality. However, if there is excessive phosphate in the water, it causes algae to grow drastically faster than the natural ecosystems can manage. It could lead to digestive problems that may occur from extremely high levels of phosphate. As for drinking water sources, it can be harmful, even at low levels.

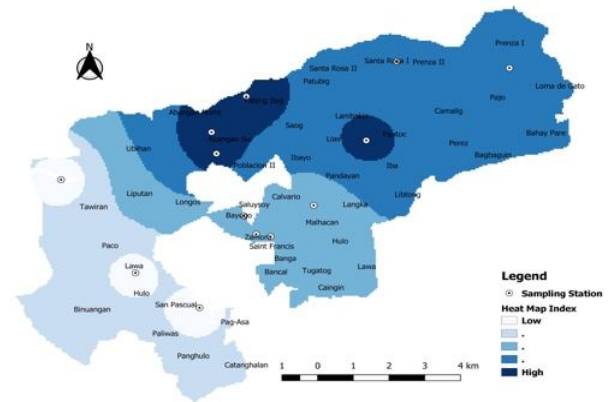


Figure: 11 Phosphates Spatial Distribution

Another indicator of good quality of the river is the transparency of water which is directly affected by the amount of sunlight available, also suspended particles in the water column and the sufficient amount of dissolved solids specifically the colored dissolved organic material (CDOM) which is always present in the water. Alongside, the mere presence of salt ions can cause suspended particles to be aggregate and settle even at the extremely base of a waterway and for this situation that is of the river.

In Figure. 12, the TSS spatial distribution is drawn weightily in the dense area of this water quality parameter.

Remarkably, the focal point of the strength is at the very core of the sampling stations.

From the spatial distribution map Figure. 12, the deficiency of TSS in the river water is observed in Lawa and Hulo in Obando, and in some sampling stations of Marilao like Loma De Gato, Santa Rosa, Prenza I and II having below the permissible limit. Consequently, high concentrations of TSS past the limit may cause numerous issues for stream wellbeing and aquatic life. In a maximum dire outcome imaginable, having High TSS in a water body, for example, may frequently mean higher convergences of as well as microorganisms, supplements, pesticides, and metals in the water.

A considerable number of studies mainly concentrating on explore concentrating to water nature of water bodies from prominent transboundary rivers like MMORS hydrographical and areas of concern are minimal, with that being said this study has a great importance indeed for the very reason that it not only limited to describing the suitability of surface water sources from this hydrographical region for human utilization yet, in addition, it tends to be expanded

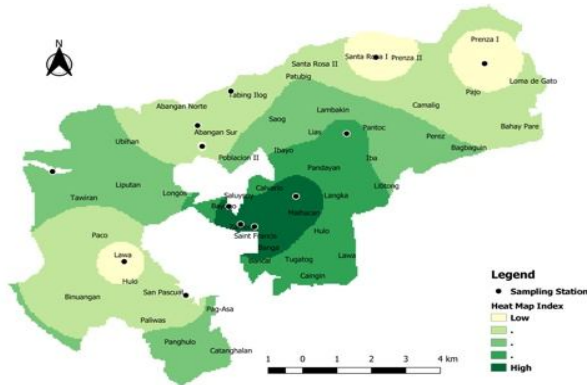


Figure 12: TSS Spatial Distribution

For correspondence of generally speaking water quality data to the competent authorities and policymakers. This is reflected in the spatial distribution of the overall pollution index which is illustrated in the following Figure. Figure. 13 simply bears witness to that practically 80% of the sampling stations generally of Meycauayan and Marilao are hugely dirtied in the wake of experiencing test results to anticipate the whole MMORS condition with its comparing water contamination level classification indicated as 'Very Poor' whereas Obando river area which is nearly 20% of the remaining in the heat map is graded as 'Poor.'

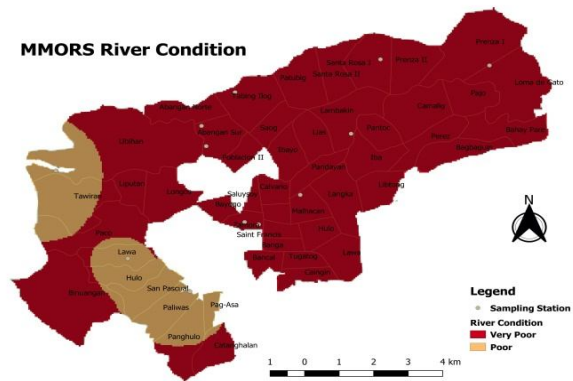


Figure 13: MMORS Water Quality

4. CONCLUSION

This study is able to present a working model from DENR-EMB Region 3. Based on the KDE heat map interpolation of the different water parameters and WQI result spatial distribution, most of the sampling station is incredibly polluted, provided that they have 'Poor' and 'Poor' condition as saw in the past Figure.

The author recommends that this study and the result should also be adopted for future research in other provinces and regions to become the basis of different local governments to lobby, craft, and execute ordinances and policies that will rectify and eradicate illegal practices. This can only be achieved through proper dissemination of results to local officials by tapping them on the real situation.

The use of visualizing a data-driven approach with the help of the GIS-based model in providing pollution prediction it is now viable to do such regardless of the water parameter of a particular river system. It can be a big help to the community of Bulacan. It can also be implemented on various major river systems across the Philippines.

ACKNOWLEDGMENT

The author acknowledges DENR-EMB Region 3 for providing the historical dataset of MMORS. And the Commission on Higher Education (CHED) for the funding of this study.

REFERENCES

1. Blacksmith Institute, "The World's Worst Polluted Places: The Top Ten," 2007.
2. M. C. Malenab, E. Visco, D. Geges, J. M. Amparo, D. Torio, and C. E. Jimena, "Analysis of the Integrated Water Resource Management in a Water Quality Management Area in the Philippines : The Case of Meycauayan-Marilao-Obando River System," vol. 98, no. December, pp. 84–98, 2016.
3. C. Li, "Preprocessing Methods and Pipelines of Data Mining: An Overview," no. June, pp. 1–7, 2019.

4. N. El-Jabi, D. Caissie, and N. Turkkan, “**Water Quality Index Assessment under Climate Change**,” *J. Water Resour. Prot.*, vol. 06, no. 06, pp. 533–542, 2014.
<https://doi.org/10.4236/jwarp.2014.66052>
5. R. Abrahão, M. Carvalho, W. R. Da Silva, T. T. V. Machado, C. L. M. Gadelha, and M. I. M. Hernandez, “**Use of index analysis to evaluate the water quality of a stream receiving industrial effluents**,” *Water SA*, vol. 33, no. 4, pp. 459–465, 2007.
6. R. Paje and J. M. Cuna, “**Department of Environment and Natural Resources**,” in *Water Quality Guidelines and General Effluent Standard of 2016*, D. A. O. N. 2016-08, Ed. Department of Environment and Natural Resources, 2016, p. 03.
7. A. H. M. J. Alobaidy, H. S. Abid, and B. K. Maulood, “**Application of Water Quality Index for Assessment of Dokan Lake Ecosystem, Kurdistan Region, Iraq**,” *J. Water Resour. Prot.*, vol. 02, no. 09, pp. 792–798, 2010.
<https://doi.org/10.4236/jwarp.2010.29093>
8. S. K. Pathak, S. Prasad, and T. Pathak, “**Determination of Water Quality Index River Bhagirathi in Uttarkashi, Uttarakhand, India**,” *Soc. Issues Environ. Probl.*, vol. 3, no. 2007, pp. 3–9, 2015.
9. C. R. Ramakrishnaiah, C. Sadashivaiah, and G. Ranganna, “**Tumkur District : Census 2011 data**,” *E-Journal Chem.*, vol. 6, no. October 2006, pp. 523–530, 2011.
10. N. Rosli, A. M. M. Pazi, S. Gandaseca, N. L. A. Wahab, and P. H. Zaki, “**Comparison of Water Quality Status of Disturbed and Undisturbed Mangrove Forest at Awat-Awat Lawas Sarawak**,” *Open J. For.*, vol. 06, no. 01, pp. 14–18, 2015.
11. O. Altansukh and G. Davaa, “**Application of Index Analysis to Evaluate the Water Quality of the Tuul River in Mongolia**,” *J. Water Resour. Prot.*, vol. 03, no. 06, pp. 398–414, 2011.
<https://doi.org/10.4236/jwarp.2011.36050>
12. P. Weerakoon, “**GIS Integrated Spatio-Temporal Urban Growth Modelling: Colombo Urban Fringe, Sri Lanka**,” *J. Geogr. Inf. Syst.*, vol. 09, no. 03, pp. 372–389, 2017.
13. M. Azhar *et al.*, “**Towards a Remote Sensing and GIS-Based Technique to Study Population and Urban Growth: A Case Study of Multan**,” *Adv. Remote Sens.*, vol. 07, no. 03, pp. 245–258, 2018.
14. S. Subramani, T.; Krishnan and P. K. Kumaresan, “**Study of Groundwater Quality with GIS Application for Coonoor Taluk in Nilgiri District**,” *Int. J. Mod. Eng. Res.*, vol. 2, no. 3, pp. 586–592, 2012.
15. S. Chainey, L. Tompson, and S. Uhlig, “**The Utility of Hotspot Mapping for Predicting**,” pp. 4–28, 2008.
16. S. Chainey, “**Examining the influence of cell size and bandwidth size on kernel density estimation crime hotspot maps for predicting spatial patterns of crime**,” *BSGLg*, vol. 60, no. 1, pp. 7–19, 2013.
17. T. Hart and P. Zandbergen, “**Kernel density estimation and hotspot mapping: Examining the influence of interpolation method, grid cell size, and bandwidth on crime forecasting**,” *Policing*, vol. 37, no. 2, pp. 305–323, 2014.
18. C. Yen-Chi, “**Lecture 6: Density Estimation: Histogram and Kernel Density Estimator**,” pp. 1–11, 2018.
19. A. Gramacki, “**Kernel Density Estimation**,” pp. 25–62, 2017.
https://doi.org/10.1007/978-3-319-71688-6_3
20. G. Pezzuchi, “**A Brief Commentary on ‘The Utility of Hotspot Mapping for Predicting Spatial Patterns of Crime’**,” *Secur. J.*, vol. 21, no. 4, pp. 291–292, 2008.
<https://doi.org/10.1057/sj.2008.6>